

Possibility to Measure Polarized Gluon Distribution Via Real Gamma Beam

A. ÇELİKEL

Ankara Univ., Faculty of Sciences, Physics Dept.,
Tandoğan, Ankara - TURKEY

Abstract

We propose an experiment to measure the polarized gluon and quark distributions in scattering of polarized real γ beam on polarized nuclear target.

My report is not directly related to the topic of this workshop, namely TeV scale machines and physics. However, the method of obtaining high energy gamma beam is the same. Our proposal deals with one of the main problems of relatively low energy physics. Once upon a time it was thought that the proton's spin comes simply from adding up the spins of the quarks. A decade ago combined SLAC and EMC data for the first moment of polarized structure function of proton $g_1^p(x, Q^2)$, lead to

$$\int_0^1 g_1^p(x, Q^2) dx = 0.126 \pm 0.01$$

a rather small value. In the naive parton model, assuming the validity of Bjorken sum rule

$$\int_0^1 [g_1^p(x, Q^2) - g_1^n(x, Q^2)] dx = \frac{1}{6} \frac{g_A}{g_V}$$

and of the SU(3) analysis, this result led to following values

$$\Delta u = 0.78 \pm 0.06, \Delta d = -0.47 \pm 0.06, \Delta s = -0.19 \pm 0.06$$

$$\Delta \Sigma = \Delta u + \Delta d + \Delta s$$

for the polarized quark moments. Since then, measurements [1] have shown that only about 25 % of the spin is carried by valence quarks and much of the remaining spin must be due to the gluons which hold the proton together and to angular momentum of quarks and gluons,

$$\frac{1}{2} = \frac{1}{2} \Delta \Sigma + \Delta G + \Delta l_z$$

To obtain a full experimental information about the spin composition of nucleon, we need more and better experiments. Many theoretical papers have suggested experiments to access to ΔG . Most of these proposals will not be able to measure the gluon distribution alone: the proposal [2] will measure the product of quark and gluon distributions, [3] product of two gluon distributions, [4] product of quasi-real photon and gluon distributions. We propose to directly measure the polarized gluon distribution in the scattering of polarized real gamma beam on polarized nuclear target [5, 6].

1. Polarized Gamma Beam Formation

Nowadays high energy electron beams are available from ring (LEP, TRISTAN, HERA) and linear (SLAC) accelerators within the energy range $E_e = (30 - 50)$ GeV. LEP2 will give opportunity to reach $E_e = 100$ GeV. Higher energies up to 1 TeV will be achieved at future linear machines. Modern accelerator technology allows to get about 70% longitudinal polarization of electrons in ring and possibly higher value of polarization in linacs. Main parameters of electron beams for present and proposed machines are given in Table 1 and Table 2.

The electron beam coming from these machines can be converted into high energy photon beam via collision with laser photons with energy ω_0 . Cross sections and kinematics for Compton backscattering of laser photons off high energy electrons have been widely discussed [7]. For convenience, I write down the related formulae. The normalized differential Compton cross section is

$$\frac{1}{\sigma_c} \frac{d\sigma_c}{d\omega} = f(\omega) = \frac{1}{E_e \sigma_c} \frac{2\pi\alpha^2}{\kappa m_e^2} \left[\frac{1}{1-y} + 1 - y - 4r(1-r) + \lambda_e \lambda_0 r \kappa (1-2r)(2-y) \right] \quad (1)$$

where $y = \omega/E_e$, $r = y/[\kappa(1-y)]$, $\kappa = 4E_e\omega_0/m_e^2$, ω is the energy of the backscattered photon, λ_e and λ_0 are helicities of initial electron and laser photon. The total Compton cross section and helicity of the backscattered photon are given by

$$\begin{aligned} \sigma_c &= \sigma_c^0 + \lambda_e \lambda_0 \sigma_c^1 \\ \sigma_c^0 &= \frac{\pi\alpha^2}{\kappa m_e^2} \left[\left(2 - \frac{8}{\kappa} - \frac{16}{\kappa^2} \right) \ln(\kappa + 1) + 1 + \frac{16}{\kappa} - \frac{1}{(\kappa + 1)^2} \right] \\ \sigma_c^1 &= \frac{\pi\alpha^2}{\kappa m_e^2} \left[\left(2 + \frac{4}{\kappa} \right) \ln(\kappa + 1) - 5 + \frac{2}{\kappa + 1} - \frac{1}{(\kappa + 1)^2} \right] \end{aligned} \quad (2)$$

$$\lambda_\gamma(\omega) = \frac{\lambda_0(1-2r)(1-y + \frac{1}{1-y}) + \lambda_e r \kappa [1 + (1-y)(1-2r)^2]}{1-y + \frac{1}{1-y} - 4r(1-r) - \lambda_e \lambda_0 r \kappa (2r-1)(2-y)} \quad (3)$$

In Figures 1, 2 the energy distribution of backscattered photons are plotted for different values of κ and λ_e . Since the laser photons can be polarized completely, we take $\lambda_0 = 1$. Figures 3, 4 show the energy dependence of polarization degree of high energy photons for the same set of parameters κ , λ_e and λ_0 .

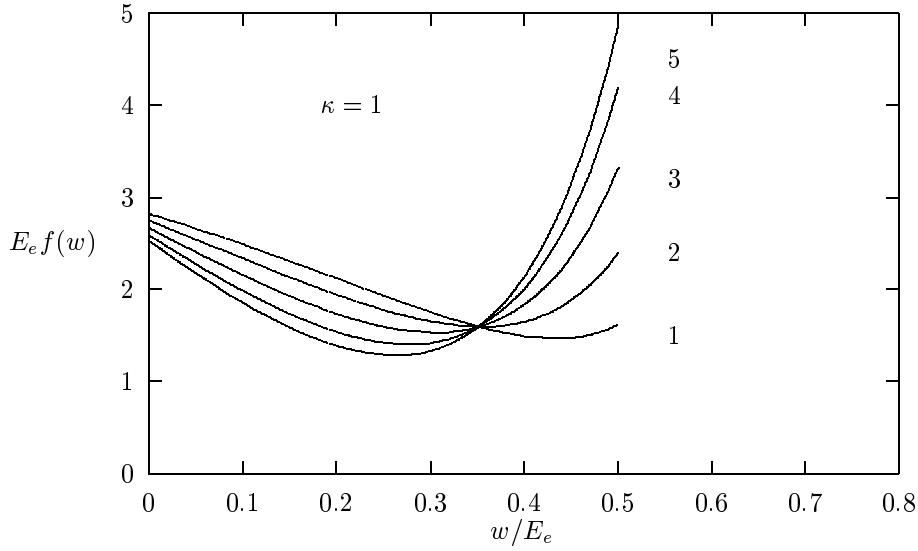


Figure 1. Energy distributions of backscattered photons. Numbers from 1 to 5 correspond to $\lambda_e \lambda_0 = 0.9, 0.5, 0.0, -0.5, -0.9$, respectively.

The photon scattering angle is a unique function of the photon energy and is given by

$$\theta_\gamma(\omega) = \frac{m_e}{E_e} \sqrt{\frac{E_e \kappa}{\omega} - (\kappa + 1)} \quad (4)$$

This dependence can be used for monochromatization of backscattered photons. At this stage, we require 1% monochromatization, i.e. $0.99\omega_{max} \leq \omega \leq \omega_{max}$. The upper limits for θ_γ obtained by using Eq.(4) will determine diameters of selecting slit. For example, taking the distance between the conversion region and absorbing wall as 100 meter, one easily obtains slit diameter $d = 360\mu m$ for LEP1 with $\kappa = 3$. As can be seen from Figures 3 and 4, the requirement of 1% monochromatization also provides nearly 100% polarization of high energy γ beam, especially in the case of opposite polarizations of electron and laser photon beams.

It should be mentioned that angular spread of backscattered photons is also influenced by that of beam electrons. A special beam gymnastic may be required to compensate this detrimental effect in particular for ring type electron accelerators.

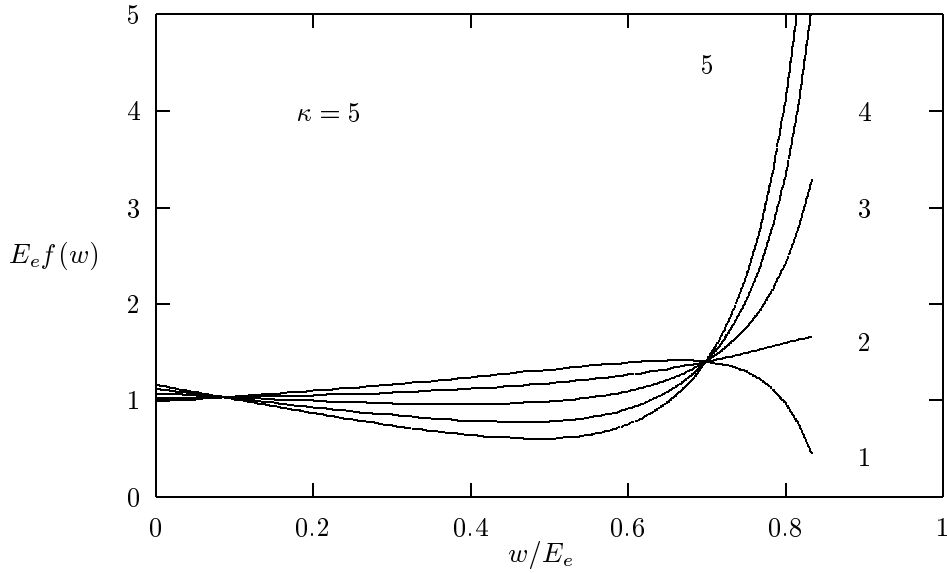


Figure 2. The same as in Fig. 1

Table 1. Main parameters of the ring electron beams.

	LEP	TRISTAN	HERA
E_e (GeV)	55 (100)	32	30 (50)
Δt_{coll} (μs)	22	5	0.096
σ_z (cm)	1.8	1.5	0.83
σ_x (μm)	200	280	280
σ_y (μm)	8	8	37
$\Delta E/E(10^{-3})$	1	2.3	0.91
$L_{lifetime}$ (hr)	20	2	10
Filling time(min)	90	40	30
$n_e(10^{10})$	41.6	22	3.65
k_b	4(8)	2	210
$2\pi R$ (km)	26.66	3.02	6.336

Table 2. Main parameters of the linear electron beams.

	E_e (TeV)	$n_e(10^{10})$	f_{rep} (Hz)	n_b	σ_x (nm)	σ_y (nm)	σ_z (μm)
SLC	0.05	3	120	1	2500	800	1000
CLIC	2.0	0.6	1700	4	90	8	170
DLC	0.5	2.1	50	172	400	32	500
JLC	0.75	0.70	150	90	260	3	80
NLC	1.0	0.65	180	90	300	3	100
TESLA	1.0	5.15	10	800	640	100	1000
VLEPP	1.0	20	300	1	2000	4	750

2. Experimental Set Up

Figure 5 shows the basic layout of the proposed experiment. Circularly polarized laser photons are scattered off electrons from a ring type or linac type accelerators. Through the process of Compton backscattering one obtains high energy photon beam which closely follows the trajectory of incoming electron beam. After conversion the electron beam should be deflected. Therefore, an additional magnet system is needed in the case of linacs. If the linac-electron beam has a multibunch structure, a mirror system should be used [8] in order to convert all bunches accelerated in one linac pulse, as shown in Figure 6. The distance between the mirrors must be equal to half of the distance among successive bunches. Each linac bunch is used once whereas the ring bunches are used repeatedly.

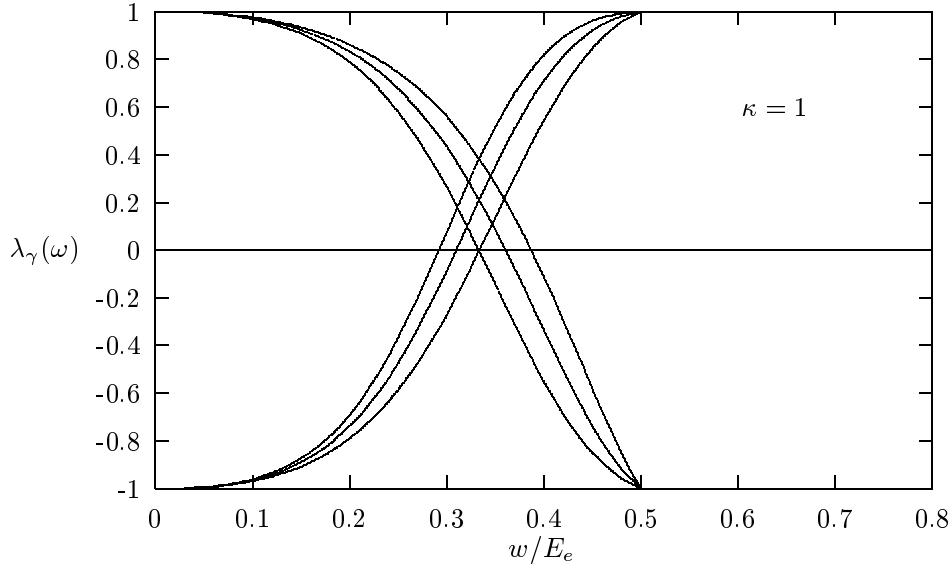


Figure 3. Helicity of backscattered photons as a function of their energy. Set of curves starting from the bottom(lower set) are plotted for $\lambda_0 = -1$ and those starting from the top (upper set) for $\lambda_0 = 1$. Lines from the left to right for lower set correspond to $\lambda_e = 0.9, 0.5, 0.0$ and for upper set $\lambda_e = 0.0, 0.5, 0.9$.

The γ beam obtained by above mentioned method, after ≈ 100 meters, will meet an absorbing wall with a tiny slit which selects hardest photons. Therefore, the diameter of the slit should be of order of a few hundred μm to reach 1% monochromatization.

Alternatively, one can keep wider slit diameter if detector is able to measure the distance between mean axis of incoming photons and interaction vertex with high precision. This will allow us to determine θ_γ from Eq.(4) and consequently the energy and polarization of interacting photons.

Behind the wall, we have almost monochromatic and fully polarized photons directed on the polarized nuclear target. The parameters of polarized targets used in high energy physics experiments are given in Table 3 [9].

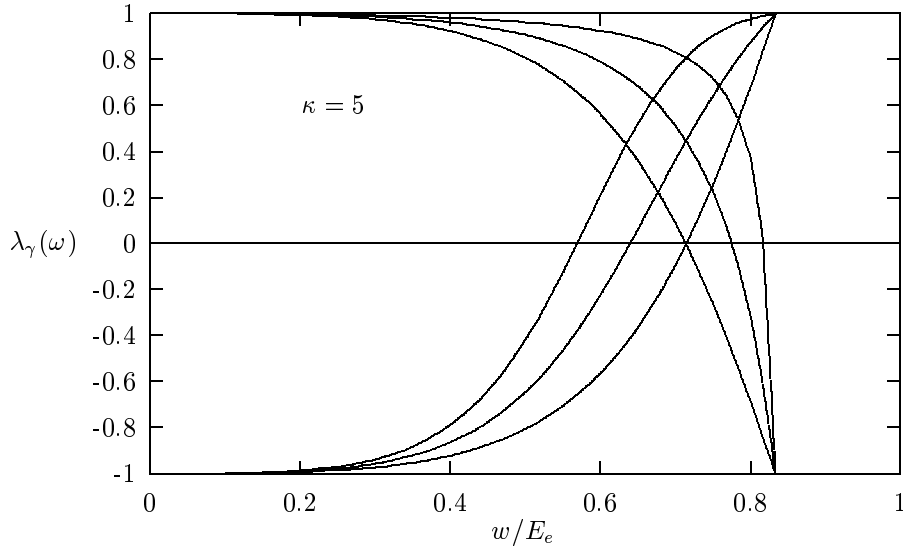


Figure 4. The same as in Figure 3

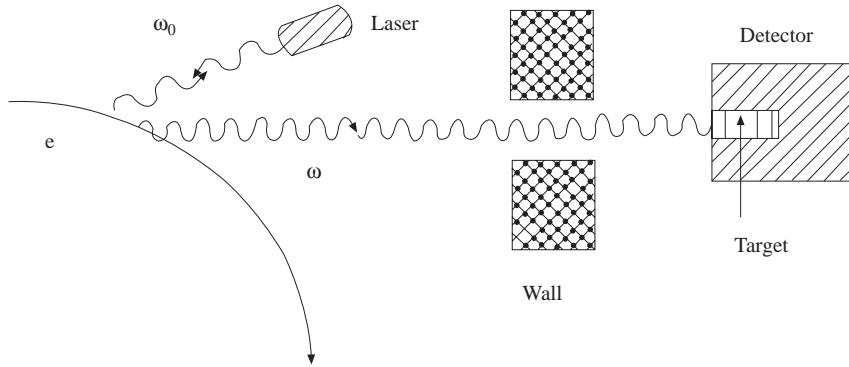


Figure 5. Schematic view of the proposed experiment.

The number of converted photons N_γ is defined by the requirement of obtaining one event in each collision with the polarized target

$$\beta N_\gamma T_n \sigma_{\gamma p} = 1 \tag{5}$$

where β is the fraction of the photons passing through the slit, T_n is the density of nucleons in the target and $\sigma_{\gamma p}$ is the total cross section of gamma-proton collision. Choosing

$0.99\omega_{max} \leq \omega \leq \omega_{max}$ yields $\beta = 0.012$ for $\kappa = 1$ and $\beta = 0.015$ for $\kappa = 3$ with LEP1 electron beam. For butanol target $T_n = 4. \times 10^{25}cm^{-2}$ and $\sigma_{\gamma p} \approx 100\mu b$ for energy under consideration, therefore one gets $N_\gamma \approx 2 \times 10^4$. Since $N_e = 4 \times 10^{11}$ for LEP1, the conversion coefficient takes the value of $k = N_\gamma/N_e = 5 \times 10^{-8}$. The corresponding values for TRISTAN and HERA are $k = 10^{-7}$ and $k = 5 \times 10^{-7}$ respectively. It should be noted that the required conversion coefficient k is small enough, therefore the upper limit imposed on kinematical parameter $\kappa \leq 4.83$ by e^+e^- pair creation in conversion region can be removed. The maximal energy of backscattered photons $\omega_{max} = \kappa E_e/(\kappa + 1)$ will increase, in principle, up to nearly electron beam energy. In this sense the situation is different from $\gamma\gamma$ [7] and γp [8] colliders.

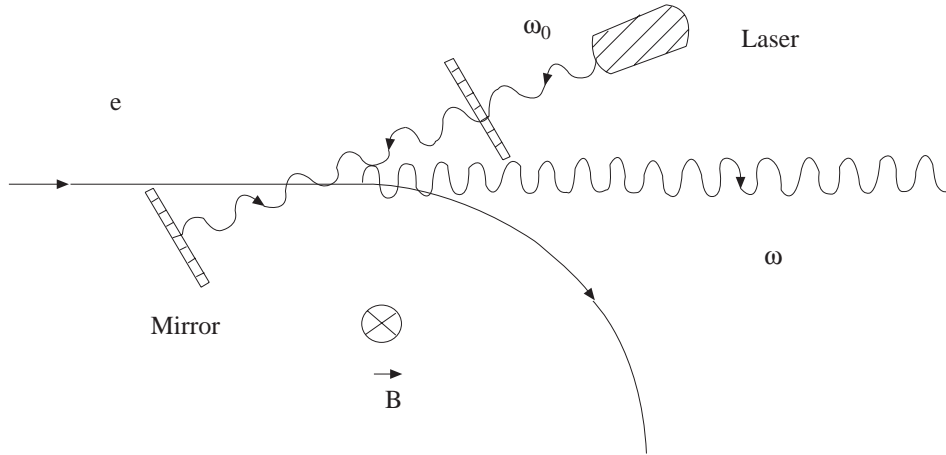


Figure 6. Close up view of the mirror system for multibunch linac.

As long as electron bunches from ring accelerators are used repeatedly, the smaller k the larger target thickness is preferable. In the linac case where each electron bunch is used once, keeping k larger may be more effective. So the polarized target with lower thickness can be chosen. For example, choosing SLAC ^3He target and electron beam from DLC yields $k = 2 \times 10^{-3}$.

One of the important aspects is the time for using up an electron bunch in ring accelerators, in other words beam life time t_b . In each collision 2×10^4 electrons have been scattered and the rest keep cycling in the ring. The LEP bunch contains 4×10^{11} electrons, so it can be repeatedly used 10^7 times. Since the collision frequency is 10^4 Hz, the bunch lasts 10^3 s before it is used up. This is comparable with filling time of LEP.

3. Laser Parameters

We are interested in three main parameters of lasers: i) Repetition rate which should be commensurable with frequency of electron bunches reaching the conversion region, ii)

The energy of laser photons which should be of the order of 1 eV and iii) Laser pulse energy which will be determined by conversion coefficient k.

For ring type electron accelerator the frequency of electron bunches reaching the conversion region is given by

$$f = \frac{c}{2\pi R} k_b \quad (6)$$

where c is the speed of light, k_b is the number of electron bunches in ring and $2\pi R$ is the circumference of the ring.

For the linac type electron accelerators frequency of laser pulses should be commensurate with f_{rep} from Table 2 and in the case of multibunch accelerator pulses mirror system should be used as mentioned above.

Table 3. Target parameters.

	Material	Pol.	Length	N/cm ²
SLAC/Yale	butanol	50-65 %	48 mm	4 10 ²⁵ nucleons
EMC	NH ₃	75-80 %	2 halves 360 mm	
Michigan	NH ₃	96%	36 mm	
SLAC E-143	¹⁵ NH ₃ & ¹⁵ ND ₃	70-75% (p) 35-40% (d)	30 mm	
Old SMC	deuterated butanol (C ₄ D ₉ OD)	>40% (d)	2 halves	
HERMES	H ³ He D	80% 50% 50%	400 mm	10 ¹⁴ atoms 9 × 10 ¹⁴ atoms 10 ¹⁴ atoms
SLAC E-142	³ He	57-64%	300 mm	7 × 10 ²¹ atoms

Let us recall the definition of the conversion factor

$$k = \frac{N_\gamma}{N_e} = \frac{A}{A_0} \quad (7)$$

where A_0 is the laser pulse energy such that each electron in a bunch is subject to collision with a laser photon and A is a pulse energy needed. The condition for each electron to be scattered once from the laser bunch is given by

$$\frac{n_0}{S_{laser}} \sigma_c = 1 \quad (8)$$

where n_0 is the number of photons in a laser pulse, S_{laser} is the transverse area of the laser bunch in the conversion region and $\sigma = 10^{-25}cm^2$ is the total Compton cross section. Since all electrons should pass through the laser bunch, it is clear that $S_{laser} \geq S_e = 4\pi\sigma_x\sigma_y$. Laser pulse energy A_0 is defined as $A_0 = n_0\omega_0$ which has the value of 320 J for LEP at $\omega_0 = 1$ eV. Because the $k=5 \times 10^{-8}$ for LEP, required pulse energy $A = 10^{-5}J$. Similar calculation can easily be done for other accelerators. The lasers having parameters almost satisfying our needs are listed in Table 4.

Table 4. List of lasers with necessary parameters for our proposal.

Type of laser	Rep. Rate (Hz)	Wavelength (nm)	Pulse length	Pulse energy(J)
Neodymium : YLF	82×10^6	527	35 psec	6
Neodymium : YAG	1-1500	1060	0.5-20 μ sec	1000
Neodymium : YAG	1-500	1060	0.3-20 μ sec	800
Neodymium : YAG	10	1060	6-8 nsec	1.1
Xe chloride	0.1-100	308	80-160 nsec	10-15
Ti-Sapphire	80×10^6	720-1080	30 psec	5×10^{-3}

4. Process Examples

Proposed experiment will give opportunity to investigate wide spectrum of polarization phenomena, starting from polarized γ -nucleon total cross section to the polarized quark and gluon distributions, including peripheric interactions, exclusive meson productions etc.

Here, we are interested in polarized parton distributions in nucleons. The main subprocesses and corresponding final states are listed in Table 5. Below we consider two processes which deal with polarized gluon distribution in some details.

Table 5. Main inclusive processes to determine parton distributions.

subprocesses	Final States
$\gamma q \rightarrow \gamma q$	$\gamma p \rightarrow \gamma j X, \gamma h X$ (h : light mesons)
$\gamma q \rightarrow gq$	$\gamma p \rightarrow jj X$
$\gamma g \rightarrow \bar{q}q$	$\gamma p \rightarrow jj X, h_1 h_2 X$
$\gamma g \rightarrow \bar{c}c$	$\gamma p \rightarrow jj X, \bar{D}DX, J/\Psi X; c \rightarrow s\mu^+ \bar{\nu}_\mu$
$\gamma g \rightarrow \bar{b}b$	$\gamma p \rightarrow jj X, \bar{B}BX, \Upsilon X; b \rightarrow c\mu^- \nu_\mu, c \rightarrow s\mu^+ \bar{\nu}_\mu$

4.1. J/ Ψ Production

The photoproduction of $c\bar{c}$ pairs via photon gluon fusion $\gamma g \rightarrow c\bar{c}$ has already been discussed ([11] and references therein). Here we reconsider this process to examine spin dependent gluon distribution. The asymmetry

$$\frac{\Delta\sigma}{\sigma} = \frac{\sigma^{\uparrow\uparrow} - \sigma^{\uparrow\downarrow}}{\sigma^{\uparrow\uparrow} + \sigma^{\uparrow\downarrow}} \quad (9)$$

provides information on $\Delta G(x, Q^2)$. The $\gamma + p \rightarrow J/\Psi + X$ production cross section in polarized case is obtained by integrating $c\bar{c}$ invariant mass over the charmonium resonance region $4M_c^2 < \hat{s} < 4M_D^2$

$$\Delta\sigma = \frac{F}{2E_\gamma M_N} \int_{4M_c^2}^{4M_D^2} d\hat{s} \Delta G(x, \hat{s}) \Delta\hat{\sigma}(\hat{s}), \quad (10)$$

and for the unpolarized case one should replace $\Delta\hat{\sigma}$ and $\Delta G(x, \hat{s})$ by $\hat{\sigma}$ and $G(x, \hat{s})$ in the above equation. The normalization factor F cancels in the asymmetry formula. Total cross sections of the subprocess $\gamma g \rightarrow c\bar{c}$ are given by

$$\Delta\hat{\sigma}(\hat{s}) = \frac{4}{9} \frac{2\pi\alpha\alpha_s(\hat{s})}{\hat{s}} \left[-\ln \frac{1+v}{1-v} + 3v \right] \quad (11)$$

$$\hat{\sigma}(\hat{s}) = \frac{4}{9} \frac{2\pi\alpha\alpha_s(\hat{s})}{\hat{s}^3} \left[(\hat{s}^2 + 4\hat{s}M_c^2 - 8M_c^4) \ln \frac{1+v}{1-v} - \hat{s}v(\hat{s} + 4M_c^2) \right], \quad (12)$$

where

$$v = \sqrt{1 - \frac{4M_c^2}{\hat{s}}}, \quad x = \frac{\hat{s}}{2E_\gamma M_N}.$$

The parametrization for the helicity difference gluon distribution function used here is [12]

$$\Delta G(x, Q_0^2) = N x^{-0.4} (1-x)^8 \quad (13)$$

where

$$N = \Delta G(Q_0^2) / \beta(0.6, 1.8) \quad (14)$$

Three sets are labeled according to values of $\Delta G(Q_0^2) = 0.5, 3.0$ and 5.7 at $Q_0^2 = 4 \text{ GeV}^2$, respectively. The distribution can be obtained at any Q^2 by evolving it with Altarelli-Parisi equations.

The results for the asymmetry for three sets of polarized gluon distributions are shown in Figure 7 as a function of E_γ . The largest value of the asymmetry is around 25% at energy $E_\gamma \approx 40 \text{ GeV}$ for set 3. Clear difference can be seen between three sets. Now let us give a rough estimation for statistical errors. The experimental data provide $\sigma(\gamma p \rightarrow J/\Psi X) \approx 5 \text{ nb}$ at $E_\gamma = 40 \text{ GeV}$ (see, for example, [13]). Using the integrated luminosity 4.5 fb^{-1} (see next subsection) one expects 2×10^7 J/Ψ events per year. If one assumes that the number of events will be reduced to 10^6 due to detection efficiency, the statistical error for $\sigma(\gamma p \rightarrow J/\Psi X)$ will be 10^{-3} . This will correspond to the value of 10^{-2} for 10% asymmetry. However, in order to observe these asymmetries the accuracy and statistics should be discussed in detail in experimental conditions.

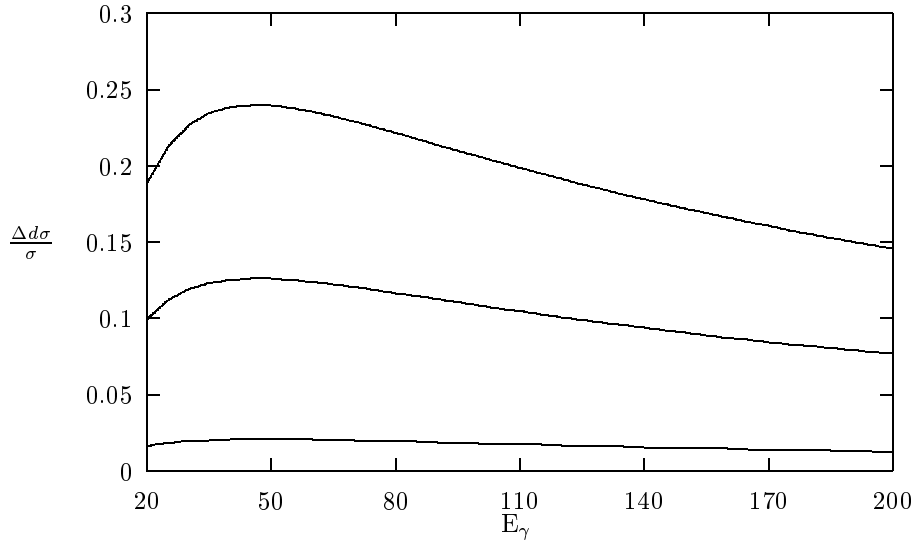


Figure 7. J/Ψ production asymmetry in polarized gamma-proton scattering for three sets of polarized gluon distributions. Curves from lowest to highest correspond to sets 1, 2 and 3, respectively.

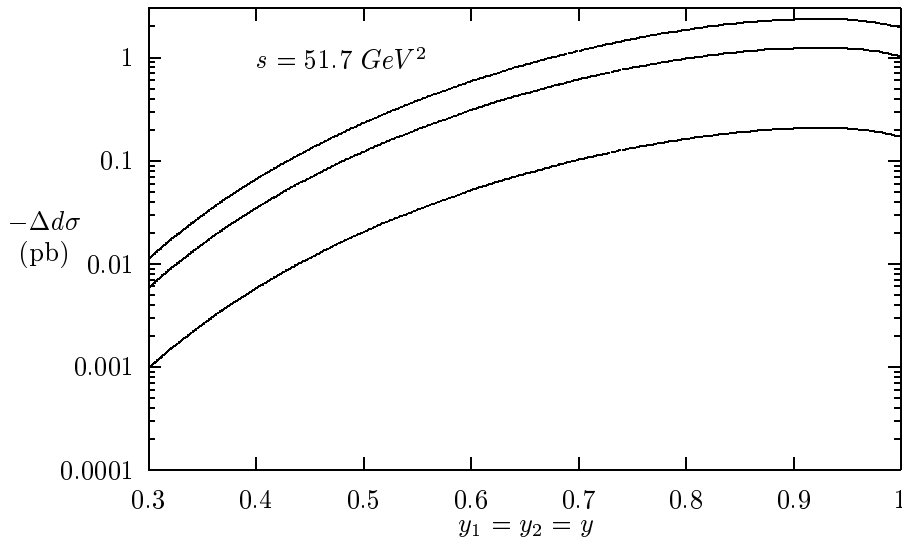


Figure 8. Integrated cross sections of the sum $\Delta(\pi) + \Delta(K)$ over the bins $1.1 < k_{T1} < 1.2$ and $1.15 < k_{2x} < 1.25$ GeV. Curve numeration is the same as in Fig. 7.

4.2. Two Hadron Production

Another process to isolate $\gamma g \rightarrow q\bar{q}$ is the production of two hadrons $\pi^+\pi^-$ (or K^+K^-) originating from light quarks u, d and s. In order to eliminate contribution of other subprocesses from photon structure the special combination of cross sections can be used [14]

$$\Delta(\pi) = \sigma(\pi^+\pi^-) + \sigma(\pi^-\pi^+) - \sigma(\pi^+\pi^+) - \sigma(\pi^-\pi^-) \quad (15)$$

$$\Delta(K) = \sigma(K^+K^-) + \sigma(K^-K^+) - \sigma(K^+K^+) - \sigma(K^-K^-) \quad (16)$$

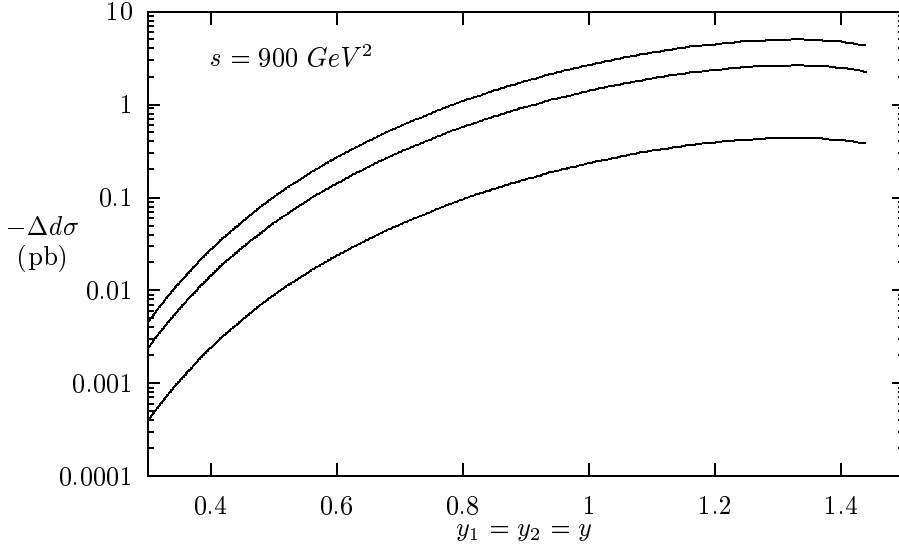


Figure 9. Integrated cross sections of the sum $\Delta(\pi) + \Delta(K)$ over the bins $2 < k_{T1} < 3$ and $2.5 < k_{2x} < 3.5$ GeV. Curve numeration is the same as in Fig. 7.

The inclusive cross section for the process $\gamma p \rightarrow h_1 + h_2 + X$ with almost monochromatic photon beam is given by

$$\sigma(h_1 h_2) = \frac{\Delta d\sigma}{dy_1 dy_2 d^2 k_{T1} dk_{2x}} = \frac{x}{\pi k_{T1}} \Delta G(x, Q_0^2) \Delta \frac{d\sigma}{d\hat{t}} \sum_q e_q^2 D_{h_1/q}(z_1) D_{h_2/\bar{q}}(z_2) \quad (17)$$

where $D_{h/q}(z)$ is the fragmentation function of light quarks with momentum fraction z of the hadron h and other definitions can be found in related references. The rapidity distribution of the integrated cross section over bins of k_{T1} and k_{2x} is the following:

$$\Delta d\sigma = \frac{\Delta d\sigma}{dy_1 dy_2 d\Phi_1}(k_{T1}, k_{2x}, s, y_1 y_2) = \int_{k_{T1}-k_0}^{k_{T1}+k_0} k'_{T1} dk'_{T1} \int_{k_{2x}-k_0}^{k_{2x}+k_0} dk'_{2x} \frac{\Delta d\sigma}{dy_1 dy_2 d^2 k'_{T1} dk'_{2x}} \quad (18)$$

In Figure 8 and Figure 9 $\Delta d\sigma$ are represented against rapidity $y_1 = y_2 = y$ for the combination of $\Delta(\pi) + \Delta(K)$ at $s=51.7 \text{ GeV}^2$ (LEP) and $s=900 \text{ GeV}^2$ (electron-linac). Both figures reflect reasonable differences among the results of three sets.

In order to estimate the number of events the integrated luminosity is needed. In our case it is given by

$$L_{int} = f_{rep} n_b 10^{35} \text{ cm}^{-2} \quad (19)$$

per working year. For linacs f_{rep} and n_b are given in Table 2, for rings f_{rep} is given by Eq.(6) and $n_b=1$. From Figure 8 and Figure 9 we obtain estimated number of events $N(y)$ at a certain rapidity value for set 3

$$L_{int} = 4.5 \text{ fb}^{-1} \quad N(y = 0.7) = 4.5 \times 10^3 \quad \text{for LEP}$$

$$L_{int} = 1 \text{ fb}^{-1} \quad N(y = 1.2) = 4 \times 10^3 \quad \text{for DLC.}$$

In certain kinematic domains event rates are sizable enough for observation. Thus detecting light mesons is a good probe to search for the polarized gluon distribution. Nevertheless, statistics and accuracy still remain to be discussed.

5. Conclusion

We show that modern accelerator and laser technologies give opportunity to prepare high energy, almost monochromatic and fully polarized γ beam with sufficiently high intensity which may be quite beneficial in investigations of polarization phenomena. In order to clarify the capability of the proposed experiment the detailed analysis of appropriate processes including detector parameters should be made.

References

- [1] J. Ashman et al., *Phys. Lett.*, **B 206** (1988) 364; B. Adeva et al., *Phys. Lett.*, **B 302** (1993) 533; P.L .Anthony et al., *Phys. Rev. Lett.*, **71** (1993) 959; D. Adams et al., *Phys. Lett.*, **B 329** (1994) 399.
- [2] E.L. Berger and J. Qiu, *Phys.Rev.*, **D 40** (1989) 778; 3128. ???
- [3] G.P. Ramsey, D. Richards and D. Sivers, *Phys. Rev.*, **D 37**(1988) 3140.
- [4] A.D. Watson, *Z. Phys.*, **C 12** (1982) 123.

- [5] S.I. Alekhin, V.I. Borodulin and S.F. Sultanov, *Inter. J. of Modern Phys.*, **A 8** (1993) 1603.
- [6] S. Atağ et al., *Europhysics Lett.*, **29** (1995) 273; *Turkish J. of Physics*, **19** (1995) 815; *Nucl. Instr. and Meth.*, **A 381** (1996) 23
- [7] I.F. Ginzburg et al., *Nucl. Instr. and Meth.*, **205** (1983) 47; *ibid.* **219** (1984) 5; V.I. Telnov, *Nucl. Instr. and Meth.*, **A 294** (1990) 72; D.I. Borden, D.A. Bauer and D.O. Caldwell, SLAC preprint SLAC-PUB-5715, Stanford (1992).
- [8] A.K. Çiftçi et al., *Nucl. Instr. and Meth.*, **A 365** (1995) 317.
- [9] G.D. Cates in SLAC-Report-444 (1994) 185.
- [10] 1994 Laser Focus World, PennWell publ., vol.29 (1994).
- [11] G. Altarelli and W.C. Stirling, *Particle World*, **1** (1989) 40; W. Vogelsang, in Physics at HERA, edited by W. Buchmuller and G. Ingelman, vol.1 (1991) 389.
- [12] S. Keller and J. Owens, *Phys. Rev.*, **D 49** (1994) 1199.
- [13] V.A. Saleev and N.P. Zotov, in Physics at HERA, edited by W. Buchmuller and G. Ingelman, vol.1 (1991) 637.
- [14] J.J. Peralta et al., *Phys. Rev.*, **D 49** (1994) 3148.